Chapter 39
Black Holes

Black holes (BH) represent the ultimate degree of compactness to which a stellar configuration can evolve. Having already called the neutron star a strange object, one cannot help labelling BH as weird. From the many fascinating aspects that are accessible via the full mathematical procedure (cf. Misner et al. 1973; Shapiro and Teukolsky 1983; Chandrasekhar 1983) we will indicate only a few points, showing that this is really a final stage of evolution, not just another late phase. We limit the description to non-rotating BH without charge.

The theoretical description to be applied is that of general relativity (see, e.g., Landau and Lifshitz 1976, vol. 2). We consider the gravitational field surrounding a very condensed mass concentration M with spherical symmetry. The vacuum solution of Einstein's field equations (2.24) for this case was found as early as 1916 by K. Schwarzschild. It gives the line element ds, i.e. the distance between neighbouring events in 4-dimensional space–time as

$$\begin{aligned} ds^2 &= g_{ij}\, dx^i\, dx^j \\ &= \left(1 - \frac{r_\mathrm{s}}{r}\right) c^2 dt^2 - \left(1 - \frac{r_\mathrm{s}}{r}\right)^{-1} dr^2 - r^2 d\vartheta^2 - r^2 \sin^2\vartheta\, d\varphi^2 \\ &= \left(1 - \frac{r_\mathrm{s}}{r}\right) c^2 dt^2 - d\sigma^2 \,, \end{aligned} \tag{39.1}$$

where one has to sum from 0 to 3 over the indices i and j, and where the usual spherical coordinates r, ϑ, φ are taken as the spatial coordinates x^1, x^2, x^3, and $x^0 = ct$. The critical parameter r_s in (39.1) is the *Schwarzschild radius*

$$r_\mathrm{s} = \frac{2GM}{c^2} \,, \tag{39.2}$$

which has the value $r_\mathrm{s} = 2.95\,\mathrm{km}$ for $M = M_\odot$. The second component of the metric tensor g_{ij}, $(1 - r_\mathrm{s}/r)^{-1}$, becomes singular at $r = r_\mathrm{s}$, but one can show that this is a non-physical singularity disappearing when other suitable coordinates are used.

R. Kippenhahn et al., *Stellar Structure and Evolution*, Astronomy and Astrophysics Library, DOI 10.1007/978-3-642-30304-3_39, © Springer-Verlag Berlin Heidelberg 2012

The proper time τ, as measured by an observer carrying a standard clock, is related to the line element ds along his world line by

$$d\tau = \frac{1}{c} ds \ . \tag{39.3}$$

For a stationary observer ($dr = d\vartheta = d\varphi = 0$) at infinity ($r \to \infty$) the proper time τ_∞ coincides with t according to (39.1). Consider two stationary observers, one at r, ϑ, φ and the other at infinity. Their proper times τ and τ_∞ are related to each other by

$$\frac{d\tau}{d\tau_\infty} = \left(1 - \frac{r_\mathrm{s}}{r}\right)^{1/2} \ . \tag{39.4}$$

Suppose that the first of them operates a light source emitting signals at regular intervals $d\tau$, for example, an atom emitting with the frequency $\nu_0 = 1/d\tau$. The other one receives the signals and measures the intervals in his own proper time as $d\tau_\infty$, i.e. he measures another frequency $\nu = 1/d\tau_\infty$. The resulting red shift due to the gravitational field is therefore

$$z \equiv \frac{\nu_0 - \nu}{\nu} = \frac{\nu_0}{\nu} - 1 = \frac{d\tau_\infty}{d\tau} - 1 = \left(1 - \frac{r_\mathrm{s}}{r}\right)^{-1/2} - 1 \ , \tag{39.5}$$

which gives $z \to \infty$ for $r \to r_\mathrm{s}$.

The metric components in (39.1) show that the 4-dimensional space–time $(x^0, \ldots, x^3)$ is curved, and this holds also for the 3-dimensional space (x^1, x^2, x^3). At the surface of a mass configuration of mass M and radius R, the Gaussian curvature K of position space can be written as

$$K = -\frac{GM}{c^2 R^3} = -\frac{1}{2}\frac{r_\mathrm{s}}{R}\frac{1}{R^2} \ . \tag{39.6}$$

This is usually very small compared with the curvature R^{-2} of the 2-dimensional surface. For example, $-K \approx 2 \times 10^{-6} R^{-2}$ at the surface of the Sun. But one already has $-K \approx 0.15 R^{-2}$ for a neutron star, and the two curvatures are comparable at the surface of a BH with $R = r_\mathrm{s}$.

Consider a test particle small enough for the gravitational field not to be disturbed which moves freely in the field from point A to B. Its world line in 4-dimensional space–time is then a *geodesic*, i.e. the length s_{AB} is an extremum. This is to say, any infinitesimal variation does not change the length:

$$\delta s_{AB} \equiv \delta \int_A^B ds = 0 \tag{39.7}$$

If the test particle moves locally with a velocity v over a spatial distance $d\sigma$, then the proper time interval $d\tau$ will be the smaller, the larger v. It becomes [cf. (39.1)]

$$d\tau = ds = 0, \quad \text{for } v = c \ , \tag{39.8}$$

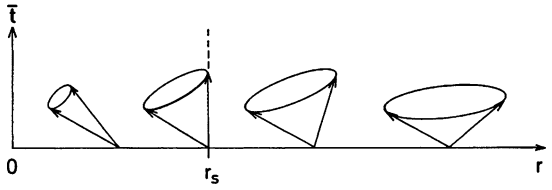

Fig. 39.1 Illustration of light cones at different distances r from the central singularity, inside and outside the Schwarzschild radius r_s

i.e. for photons or other particles of zero rest mass: they move along null geodesics. For material particles the requirement $v < c$ of special relativity (which is locally valid) means $d\tau^2$ and $ds^2 > 0$. Such separations are called *time-like.* World lines of material particles must be time-like. Separations with $ds^2 < 0$ (or $d\tau^2 < 0$) would require $v > c$; they are called *space-like.* For example, the distance between two simultaneous events ($dt = 0$) is space-like.

The null geodesies ($ds^2 = 0$), giving the propagation of photons, describe hypercones in space–time which are called *light cones.* In order to also see their properties near $r = r_s$, we introduce a new time coordinate $\bar{t}$ given by

$$\bar{t} = t + \frac{r_s}{c} \ln \left| \frac{r}{r_s} - 1 \right| , \tag{39.9}$$

which transforms (39.1) to

$$\begin{aligned} ds^2 &= \left(1 - \frac{r_s}{r}\right) c^2 d\bar{t}^2 - 2\frac{r_s}{r} c \, dr \, d\bar{t} \\ &\quad - \left(1 + \frac{r_s}{r}\right) dr^2 - r^2 d\vartheta^2 - r^2 \sin^2 \vartheta d\varphi^2 , \end{aligned} \tag{39.10}$$

which is non-singular at $r = r_s$. We consider only the radial boundaries of the light cones, i.e. the path of radially ($d\vartheta = d\varphi = 0$) emitted photons. Then (39.10) yields for $ds^2 = 0$, after division by $c^2 dr^2$, the quadratic equation

$$\left(1 - \frac{r_s}{r}\right) \left(\frac{d\bar{t}}{dr}\right)^2 - \frac{2r_s}{cr} \frac{d\bar{t}}{dr} - \frac{1}{c^2} \left(1 + \frac{r_s}{r}\right) = 0 , \tag{39.11}$$

which has the solutions

$$\left(\frac{d\bar{t}}{dr}\right)_1 = -\frac{1}{c} , \left(\frac{d\bar{t}}{dr}\right)_2 = \frac{1}{c} \frac{1 + r_s/r}{1 - r_s/r} \tag{39.12}$$

These derivatives are inclinations of the two radial boundaries of the light cone in an $r - \bar{t}$ plane (see Fig. 39.1). The first always corresponds to an inward motion with the same velocity c. The second derivative changes sign at $r = r_s$, being positive for $r > r_s$, where photons can be emitted outwards ($dr > 0$). With decreasing r, $(d\bar{t}/dr)_2$ becomes larger so that the light cone narrows and its axis turns to the left in Fig. 39.1. At $r = r_s$ the light cone is such that no photon can be emitted to the

outside ($dr > 0$). This is the reason for calling a configuration with $R = r_s$ a "black hole", and for speaking of the Schwarzschild radius r_s as the radius of a BH of mass M. For $r < r_s$ both solutions (39.12) are negative and the whole light cone is turned inwards. Therefore inside r_s all radiation (together with all material particles, which can move only inside the light cone) is drawn inexorably towards the centre. This means also that no static solution ($dr = d\vartheta = d\varphi = 0$) is possible inside r_s, since it would require a motion vertically upwards in Fig. 39.1, i.e. outside the light cone.

In order to describe the motion of a material particle, we consider all variables to depend on the parameter τ, the proper time, varying monotonically along the world line: $d\tau = ds/c$. Dots denote derivatives with respect to τ. For example, $\dot{x}^\alpha = dx^\alpha/d\tau$ is the α component of a 4-velocity. Introducing $dx^\alpha = \dot{x}^\alpha d\tau$ into (39.1) gives the useful identity

$$c^2 = g_{ij}\dot{x}^i x^j = c^2\left(1 - \frac{r_s}{r}\right)\dot{t}^2 - \left(1 - \frac{r_s}{r}\right)^{-1}\dot{r}^2 - r^2(\dot{\vartheta}^2 + \sin^2\vartheta\,\dot{\varphi}^2)\,. \tag{39.13}$$

The condition that the world line be a geodesic means that the variation $\delta s = \delta\tau = 0$, which yields the Euler–Lagrange equations

$$\frac{d}{d\tau}\left(\frac{\partial L}{\partial \dot{x}^\alpha}\right) - \frac{\partial L}{\partial x^\alpha} = 0\,, \tag{39.14}$$

with the Lagrangian L given by

$$2cL = [g_{ij}\dot{x}^i x^j]^{1/2} = \left[c^2\left(1 - \frac{r_s}{r}\right)\dot{t}^2 - \left(1 - \frac{r_s}{r}\right)^{-1}\dot{r}^2 - r^2\left(\dot{\vartheta}^2 + \sin^2\vartheta\dot{\varphi}^2\right)\right]^{1/2}. \tag{39.15}$$

From (39.13) and (39.15) follows the value $L = 1/2$. For $x^0 = ct$, (39.14) becomes simply

$$\frac{d}{d\tau}\left[\left(1 - \frac{r_s}{r}\right)\dot{t}\right] = 0\,, \quad \left(1 - \frac{r_s}{r}\right)\dot{t} = \text{constant} \equiv A\,. \tag{39.16}$$

We confine ourselves to the discussion of a radial infall ($\dot{\vartheta} = \dot{\varphi} = 0$) starting at $\tau = 0$ with zero velocity at the distance r_0. Instead of also deriving the equation of motion for $x^1 = r$ from (39.14), we simply introduce the second equation (39.16) into (39.13) and solve it for $\dot{r}$:

$$\dot{r} = c\left[A^2 - 1 + \frac{r_s}{r}\right]^{1/2}. \tag{39.17}$$

For our purposes we set $A^2 - 1 = -r_s/r_0$. According to (39.17) this means that the particle starts with zero velocity at $r = r_0$. The integration of (39.17) then yields

$$\tau = \frac{1}{2}\frac{r_0}{c}\sqrt{\frac{r_0}{r_s}}(\sin\eta + \eta)\ , \tag{39.18}$$

with the parameter $\eta = \arccos(2r/r_0 - 1)$, as can be verified by differentiation. This function $\tau = \tau(r)$ is shown in Fig. 39.2 for $r_0 = 5r_s$. Again, nothing special happens in the proper time when the particle reaches $r = r_s$. The total proper time for reaching $r = 0$ is

$$\tau_0 = \frac{\pi}{2}\frac{r_s}{c}\left(\frac{r_0}{r_s}\right)^{3/2}\ . \tag{39.19}$$

For $r_0 = 10\,r_s$ and $5\,r_s$ we have $\tau_0 = 49.67\,r_s/c$ and $17.56\,r_s/c$, respectively. These are very short times indeed, since for $M = M_\odot$ the characteristic time is only $r_s/c = 9.84 \times 10^{-6}$ s.

The motion in terms of the coordinate time t of an observer at infinity is quite different. The relation between t and τ is given by (39.16) as $d\tau/dt = (1 - r_s/r)/A$, which goes to zero when $r \to r_s$. By this relation and (39.17) one obtains a differential equation for $t(r)$, which is integrated to give

$$\frac{t}{r_s/c} = \ln\left|\frac{\xi + \operatorname{tg}\eta/2}{\xi - \operatorname{tg}\eta/2}\right| + \xi\left[\eta + \frac{r_0}{2r_s}(\eta + \sin\eta)\right]\ , \tag{39.20}$$

with η as in (39.18) and $\xi = (r_0/r_s - 1)^{1/2}$. The curve $t = t(r)$ is also shown in Fig. 39.2 for $r_0 = 5r_s$. The fact that the observer sees the τ clock of the particle slowing down completely for $r \to r_s$ has the result that $t = t(r)$ approaches $r = r_s$ only asymptotically for $t \to \infty$. Events inside $r = r_s$ are completely shielded for the distant observer by the coordinate singularity at the Schwarzschild radius acting as an "event horizon".

These few considerations may suffice to illustrate some important properties of configurations which collapse into a BH [Note that the Schwarzschild metric (39.1) is a vacuum solution, which is not valid inside the mass configuration, but holds from the surface outwards.].

As observed from the infalling surface (proper time τ) the collapse proceeds fairly rapidly and in particular quite smoothly through the Schwarzschild radius $r = r_s$. Once the surface is inside r_s a static configuration is no longer possible, and the final collapse into the central singularity within a very short time is unavoidable. This is shown by the fact that material particles have world lines only inside the local light cone, and this is open only towards $r = 0$ (even radiation falls to $r = 0$). Note that it would not help to invoke an extreme pressure exerted by unknown physical effects, since the pressure would also contribute to the gravitating energy. The singularity at $r = 0$ is an essential one (as opposed to the mere coordinate singularity at $r = r_s$) with infinite gravity, though the physical conditions there are

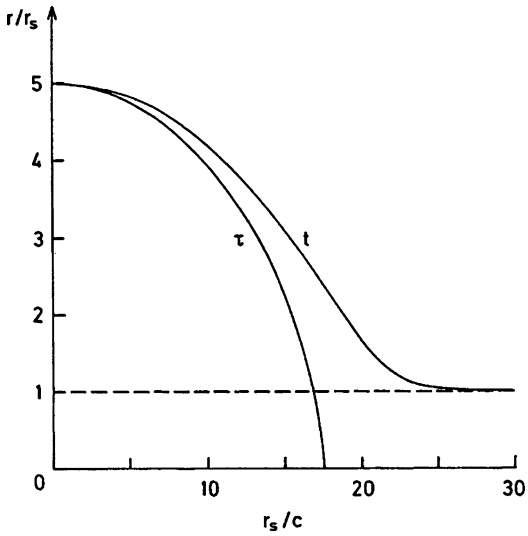

Fig. 39.2 The radial infall into a black hole for a test particle starting at a distance $5r_s$ with zero velocity. The motion is shown in terms of the particle's proper time τ, and in terms of the coordinate time t of an observer at infinity

not yet clear. Quantum effects should be included and one can speculate whether they might remove the singularity.

The collapse of a star will present itself quite differently for an astronomer who is (we hope) very far away. In his coordinate time t he will see that the collapse of the stellar surface slows down more and more, the closer it comes to r_s. In fact he will find that this critical point is not reached within finite time t; for him the collapsing surface seems to become stationary there. Of course, the approach of the surface to r_s strongly affects the light received by the distant observer. He receives photons in ever increasing intervals and with ever decreasing energy, due to the red shift $z \to \infty$ according to (39.5). Thus the collapsing star will finally "go out" for the distant observer. Only a strong gravitational field is left.

It should be mentioned that aside from the Schwarzschild solution for non-rotating, uncharged BH, there exist solutions which describe a rotating BH (Kerr metric) and a charged BH (Newman metric), the combination of these covering the full generality of possible properties of a BH: it is fully defined by mass, angular momentum, and charge. This surprising scantiness of properties left after the final collapse was summarized by Wheeler: "a black hole has no hair".

From the foregoing it is clear that black holes cannot be observed directly. However, they can be detected through their enormous influence on their surroundings. For a long time, however, BHs remained a theoretical possibility without proof of their reality. This has changed during the last few decades, and by now, their existence in two completely different mass ranges has been confirmed.

The first type of BHs are of galactic scale, sit in the centre of many galaxies, and have masses of $10^6 \lesssim M_{\rm BH}/M_\odot \lesssim 10^{10}$. They truly deserve the name *supermassive black holes*. They are detected by the analysis of the dynamics of stars in their vicinity. The overall rotation velocity (e.g. in the disks of spiral galaxies),

or the velocity dispersion (in elliptical galaxies) allows to determine the total mass interior to the galactocentric radius at which it is measured. With increasing spatial resolution of the telescopes, most notably the *Hubble Space Telescope*, the central mass could be restricted to smaller and smaller central regions, until finally only a supermassive black hole could explain the dynamics. The determined masses agree well with the estimates for the mass of the central engine in quasars and other active galaxies, needed to power the energetic of these objects.

A particularly convincing case is the Seyfert galaxy NGC 4258, where microwave emission from gas orbiting the centre has been observed. For such long wavelengths the resolution is even higher and it was found that the maser clouds orbit a central mass of forty million solar masses on orbits of only half a light year! Note that the Schwarzschild radius of such a BH is 1.2×10^{13} cm, which is still only 10^{-5} of that distance. Nevertheless, no stellar cluster with that mass could be accommodated in this volume.

Our own Milky Way is hosting a supermassive BH as well (Genzel et al. 2010). From near-infrared observations of its centre, it was found that the radio source Sgr A* coincides with a supermassive BH of about 3.6 million $M_\odot$. The proof was brought about from accurate determinations of the position and movement of a cluster of about 20 stars over a decade and longer (Eckart and Genzel 1996). As before, the stars orbit with velocities of several hundred km/s around a mass of that size which is occupying a volume with a radius smaller than 0.001 pc, and this extremely high mass concentration can only be explained with a black hole.

The origin and growth of supermassive BHs is not understood, but we have good models for the creation of the so-called *stellar black holes*. Their masses are in the range $2.5 \lesssim M_{\rm BH} \lesssim 50$, and they are thought to have been created either directly in core collapse supernova explosions (see Chap. 36, and Fig. 34.10), or by the merging of binary neutron stars. They have been detected by using the fact that in binary systems mass from a companion may flow onto the black hole, and in doing so, accumulates in an accretion disk because of the conservation of angular momentum. Due to the extremely deep gravitational potential well around the BH, the energy of the infalling material is so high that any dissipative process in the disk releases X-ray photons. X-ray binary systems are therefore the ideal place to look for proof of stellar BHs. The method is rather straightforward: one measures the orbital period Π, and the maximum line-of-sight velocity $K_{\rm comp} = v \sin i$ of the visible companion using the Doppler effect. The inclination angle is not known, but can be estimated from other information or treated with a probability approach. These two quantities are used to compute the so-called *mass function*

$$f(M_{\rm BH}, i) = \frac{K_{\rm comp}^3 \Pi}{2\pi G} = \frac{M_{\rm BH} \sin^3 i}{(1 + M_{\rm BH}/M_{\rm comp})^2}, \tag{39.21}$$

where $M_{\rm comp}$ is the mass of the companion, which has to be estimated or determined using other quantities, such as the spectral type. While there are obviously a number of uncertainties in the determination of $M_{\rm BH}$ from (39.21), there are enough X-ray

Table 39.1 Some stellar black holes (as of 2008) in X-ray binaries

Object	Π	Spect.cl.	$K_{\rm comp}$	i	$M_{\rm BH}$	$M_{\rm comp}$
V1487 Aql	33.5	K–M III	140	70	$10-18$	$1.0-1.4$
V1334 Aql	13.08211	A3–7 I	58.2		4.3 ± 0.8	12.3 ± 3.3
V404 Cyg	6.4714	K0 III–V	208.5	6.08	$10.06-13.38$	$0.5-0.8$
Cyg X–1	5.59983	O9.7 Iab	74.9	0.244	14.8 ± 1.0	$12-27$
LMC X–1	3.90917	O9–7 III	71.61		10.91 ± 1.54	31.79 ± 3.67
LS 5039	3.9060	ON6.5 V	25.2	0.0053	$2.7-5.0$	$20.0-26.3$
M33 X–7	3.453014	O7-8 III	108.9	0.777	15.65 ± 1.45	70.0 ± 6.9
V4641 Sgr	2.81730	B9 III	220.5	3.13	$6.82-7.42$	$2.92-3.26$
V1033 Sco	2.6219	F6 IV	215.5	2.73	$6.03-6.57$	$2.25-2.75$
BW Cir	2.54448	G0–5 III	279	7.34	$>7.83(50)$	$>1.02(6)$
LMC X–3	1.70479	B5 V	256.7	2.29	$9.5-13.6$	$3.0-8.3$
V381 Nor	1.5435	G8 IV–K3 II	349	6.86	$8.36-10.76$	<0.9
IC 10 X–1	1.455	WR	370	7.64	$>32.7\pm2.6$	35
IL Lup	1.116407	A2 V	129	0.25	$8.45-10.39$	$2.3-3.2$
V2107 Oph	0.521	K5 V	448	4.86	$6.64-8.30$	>0.3
GU Mus	0.432606	K3–4 V	408	3.01	$6.47-8.18$	$0.7-1.7$
V406 Vul	0.382	G5	570	7.4	$7.6-12.0$	
QZ Vul	0.344092	K3–6 V	519.9	5.01	$7.15-7.78$	$0.25-0.41$
V616 Mon	0.323016	K4 V	433	2.72	$8.70-12.86$	$0.48-0.97$
MM Vel	0.285206	K7–M0 V	475.4	3.17	$3.64-4.74$	$0.45-0.75$
V518 Per	0.212160	M4–5 V	378	1.19	$3.66-4.97$	$0.28-1.55$
KV UMa	0.169930	K7 V–M0 V	701	6.1	$6.48-7.19$	$0.22-0.32$

The orbital period Π is in days, the maximumg line-of-sight velocity $K_{\rm comp}$ in km/s, the inclination angle i in degrees, and masses in solar units
"Spect.Cl." is the spectral class of the companion, $M_{\rm comp}$ its mass
Errors in $K_{\rm comp}$ and i have been omitted, but enter into $M_{\rm BH}$ (collection courtesy of H. Ritter)

binary systems to allow a quite reliable analysis in some cases. The final argument why these central masses must be BHs is that it must be a compact object (in contrast to an ordinary star which should be visible) and that its mass is beyond the maximum allowed mass for a neutron star (Fig. 38.1). In addition, from the energy of the X-ray emission, and from the timescale of its variation one can deduce the geometric scale of the hot accretion disk. This puts further constraints on possible objects. Up to now, more than 20 BH masses have been determined (Table 39.1).

There are indications for *intermediate-mass black holes* ($50 \lesssim M_{\rm BH}/M_\odot \lesssim 10^5$), but both their existence and their origin are still a matter of discussion. They may be created either by the merging of stellar black holes, or by the collision of massive stars in massive stellar clusters. They have been postulated to explain ultra-luminous X-ray sources. For further reading on BHs and the related physics we refer to the textbook by Camenzind (2007).